

PROBING VORTEX PAIR SIZES IN THE BEREZINSKII-KOSTERLITZ-THOULESS REGIME ON A TWO-DIMENSIONAL LATTICE OF BOSE-EINSTEIN CONDENSATES

V. SCHWEIKHARD, S. TUNG, G. LAMPORESI, and E. A. CORNELL

*JILA, National Institute of Standards and Technology and University of Colorado, and
Department of Physics, University of Colorado,
Boulder, Colorado 80309-0440, USA
jilawww.colorado.edu/bec/*

We present results of a study of vortex proliferation in the Berezinskii-Kosterlitz-Thouless (BKT) regime on a two-dimensional (2D) array of Josephson-coupled Bose-Einstein condensates. In our lattice system, tunneling between nearest-neighbor condensates provides a Josephson coupling J which acts to keep the condensates' relative phases locked. A cloud of uncondensed atoms, on the other hand, interacts with the condensates and induces thermal phase fluctuations, which we observe as vortices. As long as the Josephson energy J exceeds the thermal energy T , the array is vortex-free, while with decreasing J/T , thermally activated vortices appear. We give an extended description of a time-to-length mapping technique that allows us to obtain information on the size of vortex pairs as J/T is varied.

Keywords: Vortices; Bose-Einstein condensates; Josephson-junction array.

1. Introduction

Two dimensional (2D) superfluids undergo a thermal phase transition to a normal state, which proceeds through the unbinding of vortex-antivortex pairs, i.e. pairs of vortices of opposite circulation. Our theoretical understanding of this transition is due to work by Berezinskii¹ and Kosterlitz and Thouless² (BKT). The BKT picture applies to a wide variety of 2D systems, among them Josephson junction arrays (JJA), i.e. arrays of superfluids in which phase coherence is mediated via a tunnel coupling J between adjacent sites. Placing an isolated (*free*) vortex into a JJA is thermodynamically favored if its free energy $F = E - TS \leq 0$. In an array of period d the vortex energy diverges with array size R as $E \approx J \log(R/d)$,³ but may be offset by an entropy gain $S \approx \log(R/d)$ due to the available

$\sim R^2/d^2$ sites. This leads to a critical condition $(J/T)_{crit} \approx 1$ independent of system size, below which free vortices will proliferate. In contrast, *tightly bound* vortex-antivortex pairs are less energetically costly and show up even above $(J/T)_{crit}$. The overall vortex density is thus expected to grow smoothly with decreasing J/T in the BKT crossover regime.

The BKT transition in ultracold gases has been the subject of much experimental⁴⁻⁶ and theoretical⁷⁻⁹ work, following the observation of concurrent thermal phase decoherence and vortex formation⁴ in a continuous 2D Bose gas. Our work is focused on a more detailed understanding of vortex-formation, collected in a 2D array of Bose-Einstein condensates (BECs) with experimentally controllable Josephson couplings. Parts of our results have been published previously.⁵

2. Experimental System and Procedure

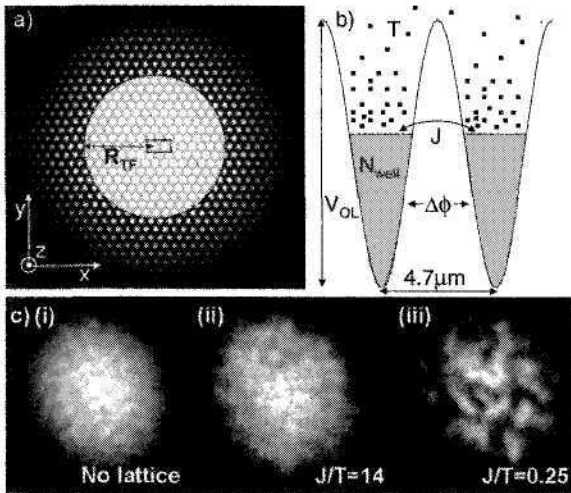


Fig. 1. (a) Experimental 2D optical lattice system. In the white-shaded area a lattice of Josephson-coupled BECs is created. The central box marks the double-well potential shown in (b). The barrier height V_{OL} and the number of condensed atoms per well, N_{well} , control the Josephson coupling J , which acts to lock the relative phase $\Delta\phi$. A cloud of uncondensed atoms at temperature T induces thermal fluctuations and phase defects in the array when $J < T$. (c) data showing thermally activated vortex formation. (i) condensate without optical lattice applied. (ii) no vortices form after application of a weak lattice with $J > T$, whereas in (iii) for $J < T$ vortices (dark spots) appear as remnants of the thermal fluctuations in the array.

We create an array of Josephson-coupled BECs by adiabatically loading a partially Bose-condensed sample of ^{87}Rb atoms into a 2D hexagonal optical lattice of period $d = 4.7\mu\text{m}$ in the x-y plane, as shown in Fig.1(a). The resulting potential barriers between adjacent sites [Fig.1(b)] rise above the condensate's chemical potential, splitting it into an array of condensates which now communicate only through tunneling. Each of the central wells contains $N_{\text{well}} \approx 7000$ condensed particles. By varying the optical lattice depth V_{OL} in a range between 500Hz and 2kHz we tune \mathbf{J} , the collective Josephson coupling, between $1.5\mu\text{K}$ and 5nK . The temperature T of the array can be adjusted between $30 - 70\text{nK}$. The "charging" energy E_c due to repulsive mean field interactions, defined in Ref. 11, is on the order of a few $p\text{K}$, much smaller than both \mathbf{J} and T . These parameters place our array in the Josephson regime, where $\mathbf{J} \gg E_c$ but $E_c \gg J/N_{\text{well}}^2$. In this regime the Josephson coupling energy $\mathbf{J}(1 - \cos(\Delta\phi))$ acts to lock the relative phases $\Delta\phi$, and if dominant will ensure at least local phase coherence in the array. A cloud of uncondensed atoms at temperature T on the other hand induces thermal fluctuations of the relative phases of order $\Delta\phi_{Th} \approx \sqrt{T/J}$. The charging energy $\frac{1}{8}E_c(\Delta N_{\text{well}})^2$ disfavors population imbalances between sites. In the Josephson regime however, with $J \gg E_c$, the resulting quantum fluctuations of the relative phase are quite negligible, of order $\Delta\phi_Q \propto (E_c/4J)^{1/4}$.

After allowing time for thermalization we probe the array. Because we do not have direct experimental access to the condensate phases in the array, we turn down the optical lattice on a time-scale t , which is fast enough to trap phase winding defects, but slow enough to allow neighboring condensates to merge, provided their phase difference is small. Phase fluctuations are thus converted to vortices in the reconnected condensate, as has been observed in the experiments of Scherer *et al.*¹² We then expand the condensate and take a destructive image in the x-y plane.

3. Earlier Results

Figure 1(c) illustrates our observations: When $J/T < 1$ vortices occur in the BEC, as remnants of the thermal fluctuations in the array. In an earlier publication⁵ we proved thermal activation as the origin of these phase fluctuations. We studied vortex activation while varying \mathbf{J} at distinct temperatures T , and showed that vortex proliferation is controlled almost exclusively by the ratio J/T , with a steep rise of vortex number around $J/T \sim 1$, just as suggested by the free energy arguments presented above.

4. Inferring Vortex-Antivortex Pair Sizes

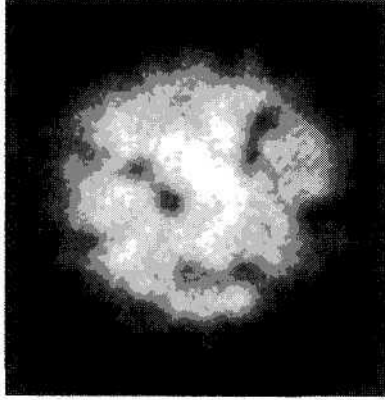


Fig. 2. Vortex-antivortex pairs, imaged just prior to their annihilation. Following the optical lattice ramp-down, tightly bound pairs annihilate faster than loosely bound pairs, providing a time-to-length mapping that allows to extract information on vortex pair sizes.

Here we describe a technique that allows us to infer vortex antivortex pair sizes. As in our earlier work we use as a robust vortex-density surrogate the "roughness" \mathcal{D} of the condensate images (see Fig. 1) caused by the vortex cores. This vortex density \mathcal{D} by itself provides no distinction between *bound* vortex-antivortex *pairs* and *free* vortices. In the following we exploit our time-dependent control of the optical potential to distinguish free or loosely bound vortices from tightly bound vortex-antivortex pairs. We make use of the fact that, once the optical lattice potential has been turned off, vortices and antivortices annihilate in the bulk condensate over a ≈ 100 ms timescale. Figure 2 shows an example image of pairs of vortices just prior to their annihilation. It is intuitively obvious that tightly bound vortex pairs will annihilate on a much faster timescale than loosely bound pairs. A "slow" optical lattice ramp-down therefore allows time for tightly bound pairs to annihilate before they can be imaged. By slowing down the ramp-down duration r [inset of Fig. 3 (a)], we can thus selectively probe vortex pairs of increasing size.

Figure 3 shows vortex activation curves, probed with two different ramp-down times.¹³ A slow ramp compared to a fast one shows a reduction of the vortex density $\mathcal{D}_<$ in arrays with fully randomized phases at low J/T . The difference directly shows the fraction of tightly bound pairs that have

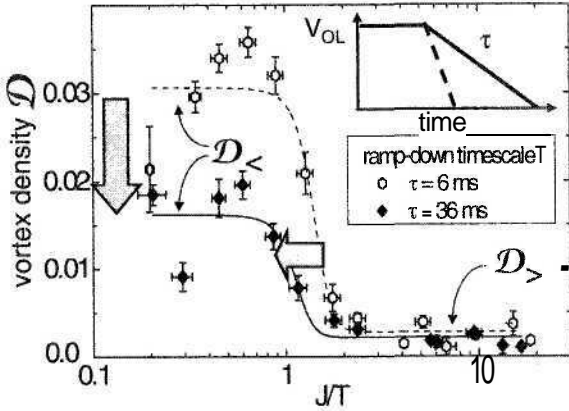


Fig. 3. Vortex density \mathcal{D} probed at different optical lattice ramp-down timescales T . A slow ramp provides time for tightly bound vortex-antivortex pairs to annihilate, allowing selective counting of loosely bound or free vortices only, whereas a fast ramp probes both free and tightly bound vortices. A fit to the vortex activation curve determines its midpoint $(J/T)_{50\%}$, its 27% - 73% width $\Delta(J/T)_{27-73}$, and the limiting values $\mathcal{D}_{<}$ ($\mathcal{D}_{>}$) well below (above) $(J/T)_{50\%}$.

annihilated on the long ramp, but not on the fast one.

To map the experimental ramp-down time-scale to theoretically more accessible vortex-antivortex pair sizes, we compare the observed number of vortices in fully randomized arrays at low J/T to simulations of vortex distributions in a hexagonal array with random phases. In these simulations, following Ref. 12, we count a vortex if all three phase differences in an elemental triangle of junctions are $\in (0, \pi)$, or if all are $G(-\pi, 0)$. A snapshot of a simulated vortex distribution is shown in Fig. 4(a). Within the central 20 lattice sites, comparable to the experimental region of interest⁵ we find, on average, a total of 10 vortices. 6 vortices occur in nearest-neighbor vortex-antivortex pairs [configuration I in Fig. 4(b)], 1.7 (0.4) occur in configuration II (III) respectively, and 1.9 occur in larger pairs or as free vortices. To relate these time-independent simulations to the experiment, we show in Fig. 4(d) the relevant cumulative vortex distributions, i.e. all vortices occurring in pairs larger than a given lower cutoff size. For a given experimental ramp-down duration, we expect only those vortex configurations to survive which are above a lower cutoff pair size imposed by the ramp-down rate.

In Fig. 4(e) we compare the simulated cumulative vortex distributions to experimentally measured vortex numbers as a function of ramp down

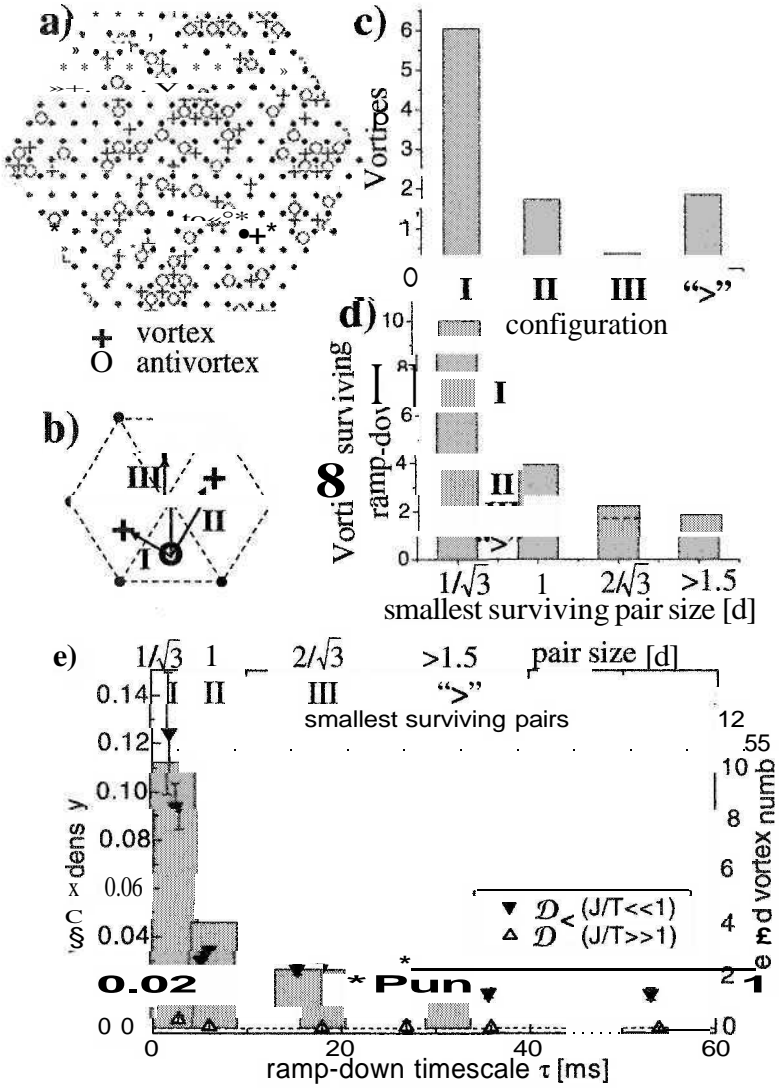


Fig. 4. Time-to-length mapping based on vortex-antivortex annihilation. (a) simulation of vortices and antivortices in array with random phases, (b) smallest possible pair sizes in a hexagonal array, I: $d/\sqrt{3}$, II: d , III: $2d/\sqrt{3}$. (c) simulated vortex pair size distribution (“>”: free vortices or pairs larger config. III), (d) cumulative distribution. (e) Mapping between ramp-down timescale T and estimated size of the smallest pairs surviving the ramp (upper axis). The difference $\mathcal{D} = \mathcal{D}_< - \mathcal{D}_>$ measures the number of observed vortices surviving the ramp (right axis). Comparison to the simulated vortex distribution yields a size estimate of the smallest surviving pairs (upper axis).

timescale, to obtain the desired time-to-length mapping. Downward triangles show the decrease of the experimentally measured saturated (low- J/T) vortex density $\mathcal{D}_<$ with increasing ramp timescale τ . The right axis shows the inferred number of vortices that survived the ramp. ≈ 11 vortices are observed for the fastest ramps, in good agreement with the *total* number of vortices expected from the simulations (indicated as grey bars). For just somewhat slower ramps of $\tau \approx 5 \text{ ms}$, only 3 vortices survive, consistent with only vortices in configuration II & III or larger remaining (indicated in Fig. 4(e), top axis). For $\tau \gtrsim 30 \text{ ms}$ ramps less than 2 vortices remain, according to our simulations spaced by more than $2d/\sqrt{3}$. Thus we infer that ramps of $\tau \approx 30 \text{ ms}$ or longer allow time for bound pairs of spacing $\lesssim 2d/\sqrt{3}$ to decay before we observe them.

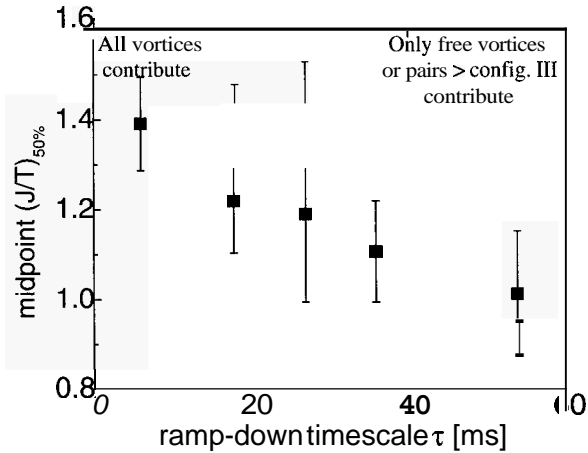


Fig. 5. A downshift in the midpoint $(J/T)_{50\%}$ of vortex activation curves such as in Fig. 3 is seen for slow ramp-down times, consistent with the occurrence of loosely bound or free vortices at lower J/T only.

With this time-to-length mapping we now return to the observations in Fig. 3. For the slower ramp we observe vortex activation at lower $(J/T)_{50\%}$, confirming that free or very loosely bound vortices occur only at higher T (lower J). In Fig. 5 we plot the midpoint $(J/T)_{50\%}$ of vortex activation curves versus the applied ramp-down time. The data quantitatively show a shift of $(J/T)_{50\%}$ from 1.4 for fast ramp times when all vortices are expected to contribute to the signal, to 1.0 for slow ramp times when only loosely bound vortices survive. The data therefore reveal that loosely bound pairs of size larger than $2d/\sqrt{3}$, or indeed free vortices, do not appear in quantity

until $J/T \leq 1.0$, whereas more tightly bound vortex pairs appear in large number already for $J/T \leq 1.4$. This result clearly illustrates the mechanism of vortex-antivortex unbinding with increasing temperature or decreasing superfluid coupling, which underlies BKT theory.

Acknowledgments

We acknowledge illuminating conversations with Leo Radzihovsky and Victor Gurarie. This work was funded by NSF and NIST.

References

1. V. Berezinskii, Sov. Phys.-JETP **32**,493 (1971); **34**,610 (1972).
2. J. Kosterlitz, D. Thouless, J. Phys. C **6**, 1181 (1973).
3. M. Tinkham, *Introduction to Superconductivity*, McGraw-Hill, Inc., New York (1996).
4. Z. Hadzibabic *et al.*, Nature **441**, 1118 (2006).
5. V. Schweikhard *et al.*, Phys. Rev. Lett. **99**, 030401 (2007).
6. P. Krüger *et al.*, Phys. Rev. Lett. **99**, 040402 (2007).
7. A. Polkovnikov *et al.*, Proc. Natl. Acad. Sci. U. S. A. **103**,6125 (2006).
8. T. Simula and P. Blakie, Phys. Rev. Lett. **96**, 020404 (2006).
9. L. Giorgetti *et al.*, Phys. Rev. A. **76**, 013613 (2007).
10. J is obtained from 3D numerical simulations of the Gross-Pitaevskii equation for the central double-well system, self-consistently including mean-field interactions of both condensed and uncondensed atoms. A useful approximation for J in our experiments is: $J(V_{OL}, N_{well}, T) \approx N_{well} \times 0.315 nK \exp[N_{well}/3950 - V_{OL}/244Hz](1 + 0.59 T/100nK)$.
11. A. Leggett, Rev. Mod. Phys. **73**,307 (2001).
12. D. Scherer *et al.*, Phys. Rev. Lett. **98**, 110402 (2007).
13. Within a dataset, the ramp-down *rate* is kept fixed, $t_r = \tau \times V_{OL}/1.3 kHz$.